

Electroweak corrections to the observables of W-boson production at RHIC

V. A. Zykunov¹

Gomel State Technical University,
October Av. 48, 246746, Gomel, Belarus;
e-mail: zykunov@ggtu.belpak.gomel.by

Abstract. The processes of the single W -production in hadron-hadron collisions are suggested for investigation of the nucleon spin. An approach is proposed for the determination of quark spin densities at low x . The lowest order electroweak radiative corrections to the observable quantities are calculated. The numerical calculations of the cross sections and the single spin asymmetries taking into consideration the electroweak corrections at RHIC energies have been made.

PACS: 12.15.Lk; 14.70.Fm; 13.88.+e

1 Introduction

Despite remarkable success in solving the proton-spin problem, which was risen by spin crisis [1], in experiments with fixed targets at CERN [2], SLAC [3] and HERMES [4] a conclusive solution to the problem of determination of u -, d -, s - quark and gluon polarizations has yet to be found. Purely inclusive measurements determining the spin structure functions for nucleons and deuteron are unfortunately restricted to probe only certain combinations of the polarized parton densities. A full analysis would require additional inputs from other measurements to separate different components. For example, semi-inclusive measurements with SMC [5] and HERMES [6] allow to access to a variety of polarized parton distributions. However, direct and separate measurements of the polarized parton distributions will remain a limited significance for some time.

Some new combinations of the polarized quark densities can be obtained from the experimental data on single spin asymmetries, when the polarized target is used in conjunction with an (un)polarized proton beam. This opportunity is offered by the dedicated RHIC spin program at BNL [7] which is supposed to start in a short period of time. Collider polarized experiments STAR and PHENIX at the RHIC energy ($\sqrt{S} \approx 500\text{GeV}$) will be the point where a high energy nucleon-nucleon spin physics will be studied by measuring a variety of spin asymmetries. Besides, there are some prospects on an acceleration of the polarized protons to 1TeV at Fermilab Tevatron [8] and these will lead to similar physics, which will be accessible to RHIC and possibly to HERA- \vec{N} [9].

In this paper we are concerned with experiments which may provide direct measurements of new independent combinations of the quark densities in polar-

ized nucleon. We will focus on inclusive single W -boson production in hadron-hadron interactions with one longitudinally polarized beam

$$N_1 + \overset{\rightarrow}{N_2} \rightarrow W^\pm + X \rightarrow l^\pm + X. \quad (1)$$

It's well known that the single spin asymmetry of the production of W -bosons via $p\vec{p} \rightarrow W^\pm X$ (e.g. A_L from Ref.[10]) is sensitive to the form of polarized quark distributions. In Sec. 2 of our paper we get formulas for single asymmetries of the process (1) for the case when in the final state only charged lepton is detected. Moreover, we will show the possibility of proposing reactions to study the polarized quark densities in the region of small x .

Radiative events originating from the loop diagrams and (as we consider the inclusive process) the processes with the emission of real photons, cannot be removed by experimental methods and so they have to be calculated theoretically and subtracted from measured cross sections of proposed reactions. In this paper the total $O(\alpha)$ electroweak radiative corrections (EWC) to the cross sections and single spin asymmetries have been calculated. In Sec. 3 and 4 we present the contributions of additional virtual and real emitted particles respectively. Numerical analysis and conclusions can be found in Sec. 5. Some technical details of calculations are presented in Appendices.

2 Born cross section and single asymmetries

The cross section for the inclusive hadronic reaction (see Fig.1,1) is given in Quark Parton Model (QPM) by conventional formula

$$d\sigma_{N_1 \vec{N}_2 \rightarrow l^\pm X} = \int dx_1 dx_2 \sum_{i,i';r1,r2} f_i^{(1),r1}(x_1, Q^2) f_{i'}^{(2),r2}(x_2, Q^2) d\hat{\sigma}_{ii'}^\pm, \quad (2)$$

where $f_i^{(a),r}(x, Q^2)$ is the probability of finding constituent i with the fraction x of the hadron's momentum and helicity r (at squared momentum transfer in the partonic reaction Q^2) in hadron a and $d\hat{\sigma}_{ii'}^\pm$ is the cross section for the elementary process leading to the final state (see Fig.1). The summation runs over all contributing parton configurations and over helicities of first and second partons ($r_{1,2} = \pm 1$). The meaning of operator "hat" will be explained below.

The process of the single W -boson production in hadron-hadron collision can be described with a very good approximation by two pair of quark-antiquark subprocesses. So for the W^- production we have

$$q_i(p_1) + \bar{q}_{i'}(p_2, \eta_2) \rightarrow W^-(q) \rightarrow l^-(k_1) + \bar{\nu}(k_2), \quad (3)$$

$$\bar{q}_i(p_1) + q_{i'}(p_2, \eta_2) \rightarrow W^-(q) \rightarrow l^-(k_1) + \bar{\nu}(k_2), \quad (4)$$

and for W^+ one

$$q_i(p_1) + \bar{q}_{i'}(p_2, \eta_2) \rightarrow W^+(q) \rightarrow l^+(k_1) + \nu(k_2), \quad (5)$$

$$\bar{q}_i(p_1) + q_{i'}(p_2, \eta_2) \rightarrow W^+(q) \rightarrow l^+(k_1) + \nu(k_2). \quad (6)$$

Our notations are the following (see Fig.1,2): p_1 is a 4-momentum of a first unpolarized (anti)quark with flavor i and mass m_1 ; p_2 is a 4-momentum of a second (anti)quark with flavor i' (i' denotes the weak isospin partner of the quark i), mass m_2 and polarization vector η_2 ; k_1 is a 4-momentum of a final charged lepton l^- or l^+ with mass m_l ; k_2 is a 4-momentum of (anti)neutrino, $q = p_1 + p_2$ is a 4-momentum of the W -boson with mass m_W . We use the standard set of Mandelstam invariants for the partonic elastic scattering

$$s = (p_1 + p_2)^2, \quad t = (p_1 - k_1)^2, \quad u = (k_1 - p_2)^2. \quad (7)$$

Squaring the matrix elements of partonic subprocess and (we use the covariant expression for the polarization vector of i' parton from [11]) we get the invariant parton-parton cross section in the Breit-Wigner form

$$d\sigma_{ii'}^\pm = \frac{\alpha^2}{4N_c s_w^4} \frac{|V_{ii'}|^2 B_{ii'}}{s((s - m_W^2)^2 + m_W^2 \Gamma_W^2)} \delta(p_1 + p_2 - k_1 - k_2) \frac{d^3 k_1}{k_{10}} \frac{d^3 k_2}{2k_{20}}, \quad (8)$$

where

$1/N_c = 1/3$ is a color factor, $s_w = \sqrt{1 - c_w^2}$ is a sine of the weak mixing angle, $c_w = m_W/m_Z$, m_Z is the Z -boson mass, Γ_W is the W -boson width, $V_{ii'}$ is Cabibbo-Kobayashi-Maskawa mixing matrix,

$$B_{ii'} = \begin{cases} u^2(1 - r_2 p_{N_2}) & \text{for (3) subprocess,} \\ t^2(1 - r_2 p_{N_2}) & \text{for (4) subprocess,} \\ t^2(1 + r_2 p_{N_2}) & \text{for (5) subprocess,} \\ u^2(1 + r_2 p_{N_2}) & \text{for (6) subprocess,} \end{cases}$$

and p_{N_2} is the degree of longitudinal polarization of a second hadron such that $p_{N_2} = \pm 1$.

The integration w.r.t. 4-momenta of unobservable (anti)neutrino gives

$$\int \frac{d^3 k_2}{2k_{20}} \delta(p_1 + p_2 - k_1 - k_2) = \delta(s + t + u - m_1^2 - m_2^2 - m_l^2). \quad (9)$$

Then in accordance with QPM we substitute $p_{1(2)} \rightarrow x_{1(2)} P_{1(2)}$, where $P_{1(2)}$ is 4-momenta of initial nucleons with masses m_N , $x_{1(2)}$ is the fraction of the first (second) nucleon momentum that is carried by the incoming quarks. We shall denote this procedure by operator "hat". Then we multiply by the parton densities of first and second hadrons, sum over helicities of quarks and integrate over x_1 , x_2 according to formula (2).

Let us introduce the Mandelstam variables for hadronic reaction

$$S = 2P_1 P_2, \quad T = -2P_1 k_1, \quad U = -2P_2 k_1, \quad (10)$$

(then $\hat{s} = x_1 x_2 S + m_1^2 + m_2^2$, $\hat{t} = x_1 T + m_1 m_N + m_l^2$, $\hat{u} = x_2 U + m_2 m_N + m_l^2$) and integrate w.r.t. x_2 with help of δ -function and noting that in QPM

$$\delta(\hat{s} + \hat{t} + \hat{u} - m_1^2 - m_2^2 - m_l^2) = \frac{1}{D} \delta(x_2 + \frac{x_1(T + m_N^2) + m_l^2}{D}), \quad D = x_1 S + U + m_N^2.$$

We can see that in this case $x_2 = x_2^0 \equiv -(x_1(T + m_N^2) + m_l^2)/D$ and this substitution corresponds to Born kinematics and we denote this by subscript (or superscript) "0".

Finally, let us consider the general form of the cross section of hadronic process (1). In the hadron-hadron collisions the center of parton-parton masses frame has an undetermined motion along the beam direction. Therefore we use the standard in this case variables: centre-of-mass energy (\sqrt{S}), component of the detected particle vector transverse to the beam direction ($|k_{1\perp}| \equiv k_{1T}$), and pseudorapidity (η), which approximately equals rapidity y , since in our case $m_l \ll k_{1T}$; then we have for T and U

$$T = -\sqrt{S}k_{1T}e^{-\eta}, \quad U = -\sqrt{S}k_{1T}e^{\eta}. \quad (11)$$

Integrating w.r.t. azimuth Φ (it's possible as the first initial hadron is unpolarized and the second one is longitudinally polarized) we have phase space $d^3k_1/k_{10} \Rightarrow \pi d\eta k_{1T}^2$, and hence the Born cross section has the form

$$\sigma_0^\pm = \sum_{i,i'} \int dx_1 q_i(x_1, Q^2) \Sigma_0, \quad (12)$$

where σ^\pm denotes the double differential cross section

$$\sigma^\pm \equiv \frac{d\sigma_{N_1 \xrightarrow{\rightarrow} N_2 \rightarrow l^\pm X}}{d\eta dk_{1T}^2}. \quad (13)$$

We use this abbreviation as well as the following

$$\sigma^\pm = \bar{\sigma}^\pm + p_{N_2} \Delta \sigma^\pm, \quad (14)$$

where $\bar{\sigma}^\pm(\Delta \sigma^\pm)$ is the spin averaged (polarization) part of cross section in the whole text.

The Born cross section is proportional to factor $\Sigma_0 = \Sigma(x_2^0)$, where

$$\Sigma(x_2) = \frac{\pi \alpha^2}{4N_c s_w^4} \frac{|V_{ii'}|^2 \hat{B}_{ii'}}{\hat{s}((\hat{s} - m_W^2)^2 + m_W^2 \Gamma_W^2) D} F_{i'}^{(2)}(x_2, Q^2), \quad (15)$$

In the expressions (12),(15) the combination of the quark densities for a second nucleon has the form

$$F_{i'}^{(2)}(x_2, Q^2) = \bar{q}_{i'}(x_2, Q^2) - c_{i'} p_{N_2} \Delta q_{i'}(x_2, Q^2), \quad (16)$$

where $(\Delta)q_i(x, Q^2) = f_i^+(x, Q^2)(-) + f_i^-(x, Q^2)$ are (longitudinally polarized) spin averaged quark densities, $c_{i'} = -1(+1)$ for quark(antiquark).

The form of the Born cross section (12) is convenient as the factorized part in the so-called 'soft' $O(\alpha^3)$ cross section (see Sect.3,4) and here let us present more simple expression for the Born cross section of the processes (1) as a convolution of partonic cross section with two parton distribution functions which we will use in the rest of this section

$$\sigma_0^\pm = \frac{\pi \alpha^2}{4N_c s_w^4} \sum_{i,i'} \int dx_1 \frac{|V_{ii'}|^2 \hat{B}_{ii'}^0}{\hat{s}_0((\hat{s}_0 - m_W^2)^2 + m_W^2 \Gamma_W^2) D} q_i(x_1, Q^2) F_{i'}^{(2)}(x_2^0, Q^2). \quad (17)$$

Let us define the polarization single asymmetries as normalized difference of the cross sections with specific spin configurations

$$A^{l^\pm}(\eta, k_{1T}) = \frac{\sigma^\pm(p_{N_2} = 1) - \sigma^\pm(p_{N_2} = -1)}{\sigma^\pm(p_{N_2} = 1) + \sigma^\pm(p_{N_2} = -1)} = \frac{\Delta\sigma^\pm}{\bar{\sigma}^\pm}. \quad (18)$$

Supposing that CKM matrix has diagonal form $V_{ii'} = \delta_{ii'}$ we can see that flavors of initial quarks and antiquarks are $i = d, s, b$; $i' = \bar{u}, \bar{c}, \bar{t}$ for (3) subprocess, $i = \bar{u}, \bar{c}, \bar{t}$; $i' = d, s, b$ for (4) subprocess, $i = u, c, t$; $i' = \bar{d}, \bar{s}, \bar{b}$ for (5) subprocess, $i = \bar{d}, \bar{s}, \bar{b}$; $i' = u, c, t$ for (6) subprocess. Neglecting the contributions of the heavy quarks (c, b, t) (the strange quark contribution $s\bar{u} \rightarrow W^-$ is neglected too as we suppose $V_{s\bar{u}}$ equals zero) we can write the Born single asymmetries as

$$A_0^{l^+}(\eta, k_{1T}) = -\frac{\int dx_1 (u'(x_1) \Delta \bar{d}(x_2^0) - \bar{d}'(x_1) \Delta u(x_2^0))}{\int dx_1 (u'(x_1) \bar{d}(x_2^0) + \bar{d}'(x_1) u(x_2^0))}, \quad (19)$$

$$A_0^{l^-}(\eta, k_{1T}) = A_0^{l^+}(\eta, k_{1T})(u \leftrightarrow d). \quad (20)$$

Here

$$u'(x_1) = K_t u(x_1), \bar{u}'(x_1) = K_t \bar{u}(x_1), d'(x_1) = K_u d(x_1), \bar{d}'(x_1) = K_u \bar{d}(x_1),$$

$$K_{t(u)} = \frac{\hat{t}^2(\hat{u}^2)}{\hat{s}((\hat{s} - m_W^2)^2 + m_W^2 \Gamma_W^2) D} \Big|_{x_2=x_2^0} \quad (21)$$

(we suppress the argument Q^2 in the quark distributions of formulas (19,21)).

The physically allowed region of x_1 and x_2 (see Fig 2.) is given by

$$-\frac{U + m_N^2 - m_l^2}{S + T + m_N^2} \leq x_1 \leq 1, \quad x_2^0 \leq x_2 \leq 1. \quad (22)$$

Let us remark that in the region of large x_1 and small k_{1T}/\sqrt{S} the expression x_2^0 does almost not depend on x_1 ($x_2^0 \approx -T/S$). Dividing the region of integration in (19,20) by parameter x_1^* (we can choose such a value of x_1^* in order to have well defined polarized quark densities in the region $x_1 < x_1^*$) we obtain the expression

$$\Delta u(-T/S) \int_{x_1^*}^1 dx_1 \bar{d}'(x_1) - \Delta \bar{d}(-T/S) \int_{x_1^*}^1 dx_1 u'(x_1) = \quad (23)$$

$$= A_0^{l^+}(\eta, k_{1T}) \int_{x_1^{min}}^{x_1^*} dx_1 (u'(x_1) \bar{d}(x_2^0) + \bar{d}'(x_1) u(x_2^0))$$

$$- \int_{x_1^{min}}^{x_1^*} dx_1 (\Delta u(x_2^0) \bar{d}'(x_1) - \Delta \bar{d}(x_2^0) u'(x_1))$$

and analogously for A^{l^-} by replacing $u \leftrightarrow d$.

Off-shell approach, which we used gives the possibility to investigate the polarized quark densities in the region of very small x . Really, the expression $-T/S$ under conditions of collider experiment can reach very small values, so using, for example, RHIC kinematics point $\sqrt{S} = 500\text{GeV}$, $k_{1T} = 10\text{GeV}$, $\eta = 2$

we can see that $-T/S$ does not exceed 0.0027. That minimum value of x is about one order of magnitude below the values quoted in studies where on-shell approximation for the W -boson was used.

So, equations (23) connect the polarized quark densities in the region of small x with the observable single asymmetries, combination of unpolarized quark densities and polarized quark densities in the region where they are well defined. If the three of the supplementary measurable quantities (for example double asymmetries $A_{\pm}(x, y)$ from Ref.[12] and QPM-expression for $g_1(x)$) are used, equations (23) allow to determine the low- x behavior of polarized u - and d -quark and antiquark distributions in nucleon.

3 Contribution of additional virtual particles to the cross section

To extract the reliable data on single asymmetries with high precision from hadron collider experiment, it is necessary to consider higher order electroweak radiative corrections. The final state photonic corrections to processes of W -production in unpolarized pp-collisions were calculated in Ref.[13]. More accurate calculation of these electroweak corrections have been suggested in Ref.[14], where both initial and final state radiation have been included, and the collinear singularity associated with final state photon radiation is regularized by the lepton mass. On the contrary, the collinear singularities associated with initial state radiation are subtracted and adsorbed into the parton distribution functions. Due to these results do not contain the quark masses, but depend analytically on other unphysical parameter δ_{θ} , which determines a collinear region.

In this paper we present the new explicit formulae for EWC to inclusive single W -production in polarized hadron-hadron collisions, where by analogy to the calculations of the radiative corrections to the hadron current in the deep inelastic scattering of lepton by nucleons [15, 16, 17, 18] we used a finite quark masses to regularise the collinear singularities. In Sect.5 we consider the dependence of the results on various quark masses and the comparison of them with the results for EWC, when the strategy of collinear singularity extraction has been employed.

As in final state only charged lepton is detected we use for calculation the covariant method [19], which has conclusive advantage: the results are independent of unphysical parameter – maximum soft photon energy E_{cut} (see for example Ref.[14]).

The one-loop contribution of additional virtual particles (V-contribution) has been calculated in t'Hooft-Feynman gauge and in on-mass renormalization scheme which uses α, m_W, m_Z , Higgs boson mass m_H and the fermion masses as independent parameters. The virtual one-loop diagrams are shown in Fig.3.

The cross section of V-contribution is proportional to the Born cross section and could be written as

$$\sigma_V^{\pm} = \sum_{i,i'} \int dx_1 q_i(x_1, Q^2) \hat{\delta}_V^{ii'}|_{x_2=x_2^0} \Sigma_0. \quad (24)$$

Here factor $\delta_V^{ii'}$ is polarization independent and consists of seven terms

$$\delta_V^{ii'} = \delta_W + \delta_{Vl} + \delta_{Vq}^{ii'} + \delta_{Sl} + \delta_{Sq} + \delta_{\gamma W}^{ii'} + \delta_{ZW}^{ii'}. \quad (25)$$

We do not repeat here the explicit expressions for all these contributions but instead refer the readers to Ref.[17],[20]. Let us consider the meaning of various terms in (25). The correction δ_W is the W -boson self-energy contribution (Fig.3,1), which has a slightly modified form from what is presented in Ref.[17]. This is due to resonant W boson production

$$\delta_W = 2Re \frac{s - m_W^2 - im_W \Gamma_W}{(s - m_W^2)^2 + m_W^2 \Gamma_W^2} \hat{\Sigma}_T^W(s), \quad (26)$$

where $\hat{\Sigma}_T^W(s)$ is the renormalized transverse part of the W -boson self energy (it can be found from formula (6.1) of Ref.[20]). The term δ_{Vl} is the leptonic vertex correction (Fig.3,2) (see formula (2.10) of Ref.[17]), $\delta_{Vq}^{ii'}$ is the quark vertex correction (Fig.3,3) (see formula (2.11) of Ref.[17], we left the flavour indices at this correction and boxes contributions), δ_{Sl} is the neutrino self energy contribution (Fig.3,4) (see formula (2.12) of Ref.[17]). Up-quarks self energy contribution (Fig.3,5) (down-quarks self energy contribution equals zero) is given by

$$\delta_{Sq} = -\frac{\alpha}{4\pi} \left[Q_u^2 \left(\ln \frac{m_Z^2}{m_u^2} - 2 \ln \frac{m_u^2}{\lambda^2} \right) - Q_d^2 \left(\ln \frac{m_Z^2}{m_d^2} - 2 \ln \frac{m_d^2}{\lambda^2} \right) + \frac{3}{2} \right]. \quad (27)$$

This expression is obtained from formula (5.46) of Ref.[20] (see also the remark below it).

We recalculated the box contributions through the quantities $I_{1,2}^{\gamma W}$ and $I_{1,2}^{ZW}$ of Ref.[17] and present them here to stress their dependence on flavour of quarks and the channel of reaction: γW box contribution (Fig.3,6 and Fig.3,7)

$$\delta_{\gamma W}^{u\bar{d}} = \delta_{\gamma W}^{\bar{u}d} = \delta_{\gamma W}, \quad \delta_{\gamma W}^{d\bar{u}} = \delta_{\gamma W}^{\bar{d}u} = \delta_{\gamma W}(t \leftrightarrow u, i \leftrightarrow i'), \quad (28)$$

where

$$\delta_{\gamma W} = \frac{2\alpha}{\pi} Re Q_l (Q_i I_1^{\gamma W, i}(s, t) + Q_{i'} I_2^{\gamma W, i'}(s, u)); \quad (29)$$

ZW box contribution (Fig.3,6 and Fig.3,7)

$$\delta_{ZW}^{u\bar{d}} = \delta_{ZW}^{\bar{u}d} = \delta_{ZW}, \quad \delta_{ZW}^{d\bar{u}} = \delta_{ZW}^{\bar{d}u} = \delta_{ZW}(t \leftrightarrow u, i \leftrightarrow i'), \quad (30)$$

where

$$\begin{aligned} \delta_{ZW} &= \frac{2\alpha}{\pi} Re [((v_l + a_l)(v_i + a_i) + (v_{i'} + a_{i'})(v_{i'} + a_{i'})) I_1^{ZW}(s, t) \\ &\quad + ((v_l + a_l)(v_{i'} + a_{i'}) + (v_{i'} + a_{i'})(v_i + a_i)) I_2^{ZW}(s, u)]. \end{aligned} \quad (31)$$

The vector and axial vector couplings constants v_i , a_i of the i -fermion- Z vertex are determined from the electric charge (Q_i) of fermion expressed in

units of proton's charge (e.g. $Q_u \equiv Q_{\bar{u}} = +2/3$, $Q_l = -1$) and the 3-component of the weak fermion isospin (I_i^3)

$$v_i = \frac{I_i^3 - 2s_w Q_i}{2s_w c_w}, \quad a_i = \frac{I_i^3}{2s_w c_w}.$$

Let us present the cross section of V-contribution as the sum of infrared divergent (IR) and IR-finite parts

$$\sigma_V^{\pm} = \sigma_V^{\pm, IR} + \sigma_V^{\pm, F} = \sum_{i, i'} \int dx_1 q_i(x_1, Q^2) \Sigma_0 (\hat{\delta}_V^{IR} + \hat{\delta}_V^F) |_{x_2=x_2^0}. \quad (32)$$

Infrared divergent part of V-contribution is regularized with the help of photon mass λ and for the correction δ_V^{IR} we find

$$\delta_V^{IR} = \frac{\alpha}{2\pi} \log \frac{s}{\lambda^2} J(0), \quad (33)$$

where the expression for $J(0)$ will be considered in the next section. The finite part of V-contribution cross section contains correction

$$\delta_V^F = \delta_V^{ii'} - \delta_V^{IR} = \delta_V^{ii'} (\lambda^2 \rightarrow s). \quad (34)$$

4 The photon bremsstrahlung $N_1 \vec{N}_2 \rightarrow l^{\pm} \gamma X$

In order to get infrared finite results for the hadronic process cross section we have to include the real bremsstrahlung correction (Fig.4).

The differential cross section for the partonic process with emission of one real photon reads

$$d\sigma_{q_i q_{i'} \rightarrow l \nu \gamma} = \frac{\alpha^3 |V_{ii'}|^2}{2^6 \pi^2 s_w^4 N_c} \frac{1}{s} \sum_{pol} |R|^2 \delta(p_1 + p_2 - k_1 - k_2 - k) \frac{d^3 k_1}{2k_{10}} \frac{d^3 k_2}{2k_{20}} \frac{d^3 k}{2k_0}, \quad (35)$$

where squared matrix element¹ is the sum of initial state (index i), final state (index f) and interference terms respectively

$$\sum_{pol} |R|^2 = (R_i R_i^+)^{nn'} + (R_f R_f^+)^{nn'} + (R_i R_f^+ + R_f R_i^+)^{nn'}, \quad (36)$$

$$(R_i R_i^+)^{nn'} = -\Pi_q \Pi_q^+ Sp[(G_i^{nn'})^{\mu\rho} U_{i,p}^n (G_i^{nn'}{}^T)_{\rho}^{\mu'} U_{i,a}^n] Sp[\gamma_{\mu} U_{f,a}^{n'} \gamma_{\mu'} U_{f,p}^{n'}],$$

$$(R_f R_f^+)^{nn'} = -\Pi_l \Pi_l^+ Sp[\gamma_{\mu} U_{i,p}^n \gamma_{\mu'} U_{i,a}^n] Sp[(G_f^{nn'})^{\mu\rho} U_{f,a}^{n'} (G_f^{nn'}{}^T)_{\rho}^{\mu'} U_{f,p}^{n'}],$$

¹For the calculation of matrix element we used the standard Feynman rules and the procedure of separation of diagram Fig.4,4 into the initial and final state radiation parts according to Ref.[13]. As a result, 'initial' part of our matrix element completely coincides with formula (2.14) of Ref.[13].

$$(R_i R_f^+ + R_f R_i^+)^{nn'} = -\Pi_l \Pi_q^+ (Sp[(G_i^{nn'})^{\mu\rho} U_{i,p}^n \gamma_{\mu'} U_{i,a}^n] Sp[\gamma_{\mu} U_{f,a}^{n'} (G_f^{n'}{}^T)_{\rho}^{\mu'} U_{f,p}^{n'}] \\ + Sp[\gamma_{\mu} U_{i,p}^n (G_i^{nn'}{}^T)_{\rho}^{\mu'} U_{i,a}^n] Sp[(G_f^{n'})^{\mu\rho} U_{f,a}^{n'} \gamma_{\mu'} U_{f,p}^{n'}]).$$

Indices n, n' denote the type of the processes: $n = -(+)$ for $q\bar{q}(\bar{q}q)$ initial state, and $n' = -(+)$ for $l^-\bar{\nu}(l^+\nu)$ final state, and $\Pi_l(\Pi_q)$ is a W -boson propagator in the case of the lepton(quark) bremsstrahlung

$$\Pi_l = 1/(s - m_W^2 + im_W \Gamma_W), \quad \Pi_q = -1/(s - 2kq - m_W^2 + im_W \Gamma_W) = 1/(z + t_{w\Gamma}), \\ t_{w\Gamma} = t_w - im_W \Gamma_W, \quad t_w = v - s + m_W^2, \quad q = p_1 + p_2. \quad (37)$$

As the kinematical variables of the radiated process we use in this case

$$z = 2kk_1, \quad z_1 = 2kp_1, \quad t_1 = (p_2 - k_2)^2, \quad u_1 = 2kp_2 = v + z - z_1, \\ v = 2kk_2 = s + u + t - m_1^2 - m_2^2 - m_l^2, \quad (38)$$

where k is a 4-momentum of the radiated photon.

The matrices U originate from the products of bispinor amplitudes and the expressions $(1 \pm \gamma_5)$:

$$U_{i,p}^- = (1 - \gamma_5)\hat{p}_1, \quad U_{i,a}^- = (1 + \gamma_5\hat{\eta}_2)(\hat{p}_2 - m_2), \quad U_{i,p}^+ = (1 - \gamma_5)\hat{p}_2, \quad U_{i,a}^+ = \hat{p}_1 - m_1, \quad (39)$$

$$U_{f,a}^- = (1 - \gamma_5)\hat{k}_2, \quad U_{f,p}^- = \hat{k}_1 + m, \quad U_{f,a}^+ = (1 - \gamma_5)\hat{k}_1, \quad U_{f,p}^+ = \hat{k}_2, \quad (\hat{p} = \gamma^\mu p_\mu)$$

and the matrices G originate from the fermion propagator and $WW\gamma$ -vertex:

$$(G_i^{-n'})^{\mu\rho} = Q_i \gamma^\mu \frac{2p_1^\rho - \hat{k}\gamma^\rho}{z_1} - Q_{i'} \frac{2p_2^\rho - \gamma^\rho \hat{k}}{u_1} \gamma^\mu + (G_i^{W^{n'}})_{\rho}^{\mu\rho}, \quad (40)$$

$$(G_i^{+n'})^{\mu\rho} = Q_i \frac{-2p_1^\rho + \gamma^\rho \hat{k}}{z_1} \gamma^\mu - Q_{i'} \gamma^\mu \frac{-2p_2^\rho + \hat{k}\gamma^\rho}{u_1} + (G_i^{W^{n'}})_{\rho}^{\mu\rho},$$

$$(G_f^-)^{\mu\rho} = Q_l \frac{2k_1^\rho + \gamma^\rho \hat{k}}{z} \gamma^\mu + (G_f^{W^-})_{\rho}^{\mu\rho}, \quad (G_f^+)^{\mu\rho} = -Q_l \gamma^\mu \frac{2k_1^\rho + \hat{k}\gamma^\rho}{z} + (G_f^{W^+})_{\rho}^{\mu\rho},$$

$$(G_f^{W^+})_{\mu\rho} = \gamma^\rho \frac{1}{2kq} C_{\rho\mu\rho'}^3(-k, q, k - q), \quad (G_f^{W^-})_{\mu\rho} = \gamma^{\rho'} \frac{1}{2kq} C_{\rho\rho'\mu}^3(-k, k - q, q),$$

$$(G_i^{W^+})_{\mu\rho} = \gamma^{\rho'} \frac{1}{2kq} C_{\rho\rho'\mu}^3(-k, q, k - q), \quad (G_i^{W^-})_{\mu\rho} = \gamma^{\rho'} \frac{1}{2kq} C_{\rho\mu\rho'}^3(-k, k - q, q),$$

where the matrix C^3 corresponds to $WW\gamma$ -vertex and for the minimal standard model reads

$$C_{\mu\nu\rho}^3(p^0, p^+, p^-) = g_{\rho\nu}(p^- - p^+)_\mu + g_{\mu\nu}(p^+ - p^0)_\rho + g_{\mu\rho}(p^0 - p^-)_\nu.$$

After transition to hadron-hadron cross section according to prescription of QPM, we can present the cross section of bremsstrahlung (R-contribution) by splitting it into a soft IR-part and a hard contribution [19] (we again use the abbreviation (13) for the double cross section σ^\pm)

$$\sigma_R^\pm = \sigma_R^{\pm,IR} + \sigma_R^{\pm,F}. \quad (41)$$

The infrared divergent part (the first term) of expression (41) reads (we made the substitution $dx_2 = d\hat{v}/D$)

$$\sigma_R^{\pm,IR} = \sum_{i,i'} \int dx_1 q_i(x_1, Q^2) \hat{\Sigma}_R^{IR}, \quad (42)$$

where

$$\hat{\Sigma}_R^{IR} = -\frac{\alpha}{\pi} \int_{\hat{v}_{min}}^{\hat{v}_{max}} d\hat{v} \Sigma(x_2) I[\hat{F}^{IR}]. \quad (43)$$

The procedure of integration over the photon phase space defined as $I[A]$ is described by (1) in Appendix A. And for F^{IR} , using the method of separation of IR-terms [19] we find

$$F^{IR} = Q_l^2 \frac{m_l^2}{z^2} + c_l Q_l Q_i \frac{t}{zz_1} - c_l Q_l Q_{i'} \frac{u}{zu_1} + Q_i^2 \frac{m_1^2}{z_1^2} - Q_i Q_{i'} \frac{s}{z_1 u_1} + Q_{i'}^2 \frac{m_2^2}{u_1^2}, \quad (44)$$

where

$$c_l = \begin{cases} +1 & \text{for (3) and (6) subprocesses,} \\ -1 & \text{for (4) and (5) subprocesses.} \end{cases} \quad (45)$$

Introducing $J(\hat{v}) = \hat{v} \lim_{\lambda \rightarrow 0} I[\hat{F}^{IR}]$ we obtain two parts of the soft cross section:

$$\hat{\Sigma}_R^{IR} = -\frac{\alpha}{\pi} \Sigma_0 J(0) \int_{\hat{v}_{min}}^{\hat{v}_{max}} \frac{d\hat{v}}{\hat{v}} + \frac{\alpha}{\pi} \int_{\hat{v}_{min}}^{\hat{v}_{max}} d\hat{v} (\Sigma_0 J(0)/\hat{v} - \Sigma(x_2) I[\hat{F}^{IR}]). \quad (46)$$

The second term is infrared free and lower limit of integration for it equals zero, and the first one contains infrared divergence. In the center-of-mass-system of initial hadrons the limits of integration are

$$\begin{aligned} \hat{v}_{min} &= (\vec{k} = 0) = 2\lambda k_{20} = \lambda \tilde{v}, \quad \tilde{v} \approx \frac{D^2 + TU}{D\sqrt{S}}, \\ \hat{v}_{max} &= (x_{2max} = 1) = D(1 - x_2^0) \end{aligned} \quad (47)$$

and the infrared divergent part of bremsstrahlung cross section has the form $-\alpha/\pi \Sigma_0 J(0) \log(\hat{v}_{max}/\lambda \tilde{v})$.

Summing up IR-parts of the V- and R- contributions (formulas (32) and (42)) we get

$$\begin{aligned} \sigma_R^{\pm,IR} + \sigma_V^{\pm,IR} &= \sum_{i,i'} \int dx_1 q_i(x_1, Q^2) \frac{\alpha}{2\pi} \Sigma_0 J(0) \log \frac{\tilde{v}^2 \hat{s}_0}{\hat{v}_{max}^2} \\ &+ \sum_{i,i'} \int dx_1 q_i(x_1, Q^2) \frac{\alpha}{\pi} \int_0^{\hat{v}_{max}} d\hat{v} \frac{\Sigma_0 J(0) - \Sigma(x_2) J(\hat{v})}{\hat{v}}, \end{aligned} \quad (48)$$

as a result infrared divergences completely cancel out.

During the calculation of $I[\hat{F}^{IR}]$ the following expressions are used

$$\begin{aligned} I\left[\frac{1}{z^2}\right] &= \frac{1}{m_l^2 v}, & I\left[\frac{1}{z_1^2}\right] &= \frac{1}{m_1^2 v}, \\ I\left[\frac{1}{zz_1}\right] &= -\frac{1}{vt} \log \frac{t^2}{m_l^2 m_1^2}, & I\left[\frac{1}{zu_1}\right] &= -\frac{1}{vu} \log \frac{u^2}{m_l^2 m_2^2}, \\ I\left[\frac{1}{z_1 u_1}\right] &= \frac{1}{vs} \log \frac{s^2}{m_1^2 m_2^2}, & I\left[\frac{1}{u_1^2}\right] &= \frac{1}{m_2^2 v}, \end{aligned} \quad (49)$$

and therefore $J(\hat{v})$ has the form (we remind that $\hat{v} = D(x_2 - x_2^0)$)

$$\begin{aligned} J(\hat{v}) = & Q_l^2 - c_l Q_l Q_i \log \frac{\hat{t}^2}{m_l^2 m_1^2} + c_l Q_l Q_{i'} \log \frac{\hat{u}^2}{m_l^2 m_2^2} \\ & + Q_i^2 - Q_i Q_{i'} \log \frac{\hat{s}^2}{m_1^2 m_2^2} + Q_{i'}^2. \end{aligned} \quad (50)$$

After extraction of infrared singularity from partonic process cross section and integrating over whole phase space of real photon (see Appendix A) we can present the hard contribution cross section of inclusive process $N_1 \xrightarrow{\rightarrow} N_2 \rightarrow l^\pm \gamma X$ in the form

$$\sigma_R^{\pm, F} = \sum_{i, i'} \int dx_1 dx_2 q_i(x_1, Q^2) F_{i'}^{(2)}(x_2, Q^2) \hat{\Sigma}_R^F, \quad (51)$$

where

$$\begin{aligned} \Sigma_R^F = & \frac{\alpha^3}{8s_w^4 s N_c} |V_{i'}|^2 (Q_l^2 \Pi_l \Pi_l^+ V_l + Q_l \text{Re}[\Pi_l V_{lq}] + V_q \\ & + Q_l \Pi_l \Pi_l^+ \text{Re}[V_{lw}] + \text{Re}[\Pi_l] V_{qw} + \Pi_l \Pi_l^+ V_w), \end{aligned} \quad (52)$$

and

$$\Pi_l \Pi_l^+ = 1/((s - m_W^2)^2 + m_W^2 \Gamma_W^2).$$

The subscript in V means the origin of bremsstrahlung photon: $l/q/w$ refers to the radiation from lepton (Fig.4,3) / quark (Fig.4,1 and Fig.4,2) / W -boson (Fig.4,4) legs respectively. Double subscript corresponds to the same interference term. The expressions for the quantities V can be found in Appendix B.

So, we get three terms of $O(\alpha^3)$ cross section which include radiative corrections: infrared finite part of V (and R)-contribution $\sigma_{V(R)}^{\pm, F}$ and the part $(\sigma_V^{\pm, IR} + \sigma_R^{\pm, IR})$, where infrared divergence cancelled out in the sum

$$\sigma_{EWC}^{\pm} = \sigma_V^{\pm, F} + \sigma_R^{\pm, F} + (\sigma_V^{\pm, IR} + \sigma_R^{\pm, IR}). \quad (53)$$

All of these terms depend on a second hadron polarization. This dependence is factorized in the expression $F_{i'}^{(2)}(x_2, Q^2)$, which is containing only in $\Sigma(x_2)$ and Σ_0 . Such a factorization gives the possibility to obtain the cross section of a single W -production in unpolarized nucleon-nucleon collisions by doing a simple replacement

$$F_{i'}^{(2)}(x_2, Q^2) \rightarrow q_{i'}(x_2, Q^2). \quad (54)$$

5 Discussion of numerical results and conclusions

In the following the scale of radiative corrections and their effect on the observables of the processes (1) will be discussed ². First of all we compare the numerical estimations of our formulas to the results of the calculations Ref.[14] for the unpolarized $p\bar{p} \rightarrow l^\pm X$. We have calculated (Fig.5) μ^+ transverse momentum spectrum as a function of k_{1T} for the process $p\bar{p} \rightarrow \mu^+ X$ at $\sqrt{S} = 1.8\text{TeV}$ (Tevatron kinematics). The integration over pseudorapidity ($-1.2 \leq \eta \leq 1.2$) had been done and the MRS LO 98 set of unpolarized parton distribution functions [21] are used. It can be seen from comparison of Fig. 5 and Fig.7,b of Ref.[14] the total EWC have a similar behavior: $O(\alpha^3)$ cross section in the region $25\text{GeV} < k_{1T} < 34\text{GeV}$ is a little bit higher than Born cross section; the EWC contribution to the cross section is insignificant at $k_{1T} \sim 35(37)\text{GeV}$ for Ref.[14](our) calculations; and in the region $k_{1T} > 39\text{GeV}$ the total EWC reduce the Born cross section in both approaches, so in the resonance region ($k_{1T} \sim m_W/2$) the difference between Born and $O(\alpha^3)$ cross sections is $\sim 0.004(0.003)\text{nb/GeV}$ for Ref.[14](our) calculations.

The main uncertainty for hadronic part of the EWC in our approach is the quark mass dependence. From Fig. 6 it can be seen that in the region $k_{1T} < 40\text{GeV}$ the difference between corrections at various values of quark masses is rather essential: so increasing m_u, m_d by a factor of 10 the correction decreases for ~ 0.05 . In the vicinity of $k_{1T} \sim m_W/2$ and for $k_{1T} > m_W/2$ the discussed difference does not exceed 0.02. For the calculation of $O(\alpha^3)$ cross section of Fig.5 and also for the rest analysis we used the values of the current quark masses of $m_u = 5\text{MeV}$, $m_d = 8\text{MeV}$, considering the arguments concerning the choice of these not well-defined parameters, which are discussed in Ref.[16] (page 1101, and references therein). However for quark masses of such an order a quite good correspondence with the results of calculations by the collinear singularity extraction method is reached (parameter $\delta_\theta \geq 10^{-4}$).

To estimate the scale of radiative effects and it's influence on observable quantities in the processes (1), the numerical calculations of the cross sections (Fig.7 and Fig.9), the total EWC $\delta_{l^\pm}^u$ to spin-averaged part of cross section (Fig.8)

$$\sigma_{EWC}^\pm = \bar{\sigma}_0^\pm (1 + \delta_{l^\pm}^u) + p_{N2} \Delta \sigma_0^\pm (1 + \delta_{l^\pm}^p) \quad (55)$$

and the single spin asymmetries A^{l^\pm} taking into consideration EWC (Fig.10) at typical values for future experiment STAR at the collider RHIC ($\sqrt{S} = 500\text{GeV}$, $-1 \leq \eta \leq 2$, $\Delta\Phi = 2\pi$) have been made. We used the following standard set of electroweak parameters: $\alpha = 1/137.036$, $m_W = 80.43\text{GeV}$, $m_Z = 91.19\text{GeV}$, $M_H = 300.0\text{GeV}$, the fermion masses: $m_u = 5\text{MeV}$, $m_d = 8\text{MeV}$, $m_s = 150\text{MeV}$, $m_c = 1.5\text{GeV}$, $m_b = 4.5\text{GeV}$, $m_t = 30.0\text{GeV}$; the GRV94 proton parametrization of parton distribution functions [22] for unpolarized quarks and the GRSV96 LO proton parametrization of parton spin densities [23]. We have selected for the Q^2 in these Q^2 -dependent distributions as well as in Ref.[14]

²A program of numerical calculations of the cross sections and single spin asymmetries of processes (1) (in FORTRAN) including $O(\alpha)$ electroweak corrections is available by contacting to author via e-mail

$Q^2 = m_W^2$, since trying to use for Q an explicit momentum transfer in the partonic reaction (e.g. $Q^2 = \hat{s}$ for Born and final state radiation cross sections) we have not obtained some noticeable difference for the numerical estimation of the observable quantities. And at last, as the contributions to the observables of investigated processes which have different origin are not distinguishable experimentally, we did not conduct the comparative analysis for them.

We present in Fig.7 the numerical results for the spin-averaged part of the double differential cross section as a function of k_{1T} for the different values of pseudorapidity. As we can see, for e^+ and e^- in the final state EWC are essential and increase the Born cross section in the region $k_{1T} < m_W/2$ for $\eta = -1, 0$; the EWC are not significant at small k_{1T} for $\eta > 1$, and in the region $k_{1T} \geq m_W/2$ for all values η . For μ^+ and μ^- in the final state EWC are most essential in the resonance region for $\eta = -1, 0$, and at the small k_{1T} in the case $\eta = 1.5, 2$ (EWC decrease the Born cross section).

It can be seen from Fig.8, where the corrections δ^u to spin-averaged part of Born cross sections are represented, that muon corrections are lower than that of electron (difference is approximately 0.12). This fact corresponds to a common character of EWC dependence on masses which regularize the collinear singularity (the mass m_μ is more than m_e by 2×10^2 times) and which were discussed in the beginning of this section. General features of the corrections behavior for all cases (e^\pm, μ^\pm) and for different η are the increase in the region $k_{1T} < m_W/2$, the sharp falling in the vicinity of resonance and smooth growth at $k_{1T} > m_W/2$. The corrections to transverse mass distribution, which are represented on Fig.9 of Ref.[14] have a similar behavior.

The scale and the behavior of the radiative corrections to polarization part of the Born cross section are shown in Fig.9, but as this part of the cross section is unobservable we shall not analyze it in details, and consider the influence the radiative effects to observable quantities – polarization asymmetries (19),(20). So, Fig.10 shows Born asymmetries A_0 together with the EWC corrected results. One can see that the corrections to asymmetries are significant and decrease the Born value practically in the whole investigated region except the region of small k_{1T} and large η . Let us remark that the corrections are almost independent of particle mass in the final state (m_e or m_μ). In other words the ratios of the cross sections (i.e. asymmetries) are much less sensible to the values of masses than the cross sections themselves. For the same reason the corrections to asymmetries do not depend practically on the choice of quark masses too. So, if we change the masses of the light quarks from $m_u = 5\text{MeV}$, $m_d = 8\text{MeV}$ to the extreme value $m_u = m_d = 0.33\text{GeV}$ we get a shift of radiative corrected asymmetries by less than 0.01 in a whole investigated region, and in the region $\eta = 2$, $k_{1T} = 10\text{GeV}$, which is very important for the quark density analysis at low x (see Section 1) this shift equals 0.0032(0.0021) for $\mu^-(\mu^+)$ case. Thus we can suppose that our approach to the calculation of radiative corrections to the single spin asymmetries is practically free from the quark masses uncertainty.

In conclusion we have presented the scheme to use the processes of the single W -boson production possible at hadron-hadron colliders for the investigation of the nucleon spin structure. An approach is proposed for the determination $u-$ and $d-$ quark (and antiquark) spin densities at low x by a set of the observable

quantities. The electroweak radiative corrections to the differential cross sections and the single spin asymmetries of the processes (1) are calculated. The obtained formulas do not depend on any parameters of the infrared divergence extraction (e.g. maximum soft photon energy). We checked that EWC to asymmetries do practically not depend on the masses of the quarks which regulate in our approach the collinear singularity. Our results can be used for studies of nucleon spin at hadron-hadron colliders (RHIC and HERA). An analysis of the numerical results for the collider experiment STAR at RHIC shows that the radiative corrections prove to be important.

6 Acknowledgments

Author wishes to thank A.N.Ilychev for the assistance in calculation of the scalar integrals from Appendix A.

A Phase space of photon and scalar integrals

The integral over phase space of the radiated photon can be presented in the form

$$\begin{aligned} I[A] &= \frac{1}{\pi} \int \frac{d^3 k}{k_0} \delta[(p_1 + p_2 - k_1 - k)^2] [A] \\ &= \frac{1}{\pi} \int_{z_{min}}^{z_{max}} dz \int_{u_1_{min}}^{u_1_{max}} \frac{du_1}{\sqrt{R_{u_1}}} [A], \end{aligned} \quad (1)$$

where $-R_{u_1}/16 = \Delta_4$ is the Gramm determinant, $R_{u_1} = -A_{u_1}u_1^2 - 2B_{u_1}u_1 - C_{u_1}$ with the following coefficients:

$$\begin{aligned} A_{u_1} &= (s - v)^2 - 2(s + v)m_l^2 + m_l^4, \\ B_{u_1} &= [(s - v)(u - m_l^2) + m_l^2(2v - t - m_1^2 + 2m_2^2)]v \\ &\quad - [(s - m_l^2)(m_2^2 - t) + (u + m_1^2 - 2m_2^2 - 2m_l^2)v]z, \\ C_{u_1} &= [(v - t + m_2^2)z + (u - m_l^2)v]^2 - m_2^2v[4z^2 \\ &\quad - 2z(s - u - 2v + m_1^2 - m_l^2) + v(2u - m_2^2 + 2m_l^2)]. \end{aligned} \quad (2)$$

The limits of the double integration $u_1^{max/min}$ and $z^{max/min}$ are the roots of equations $R_{u_1} = 0$ and $u_1^{max} = u_1^{min}$ respectively

$$u_1^{max/min} = -\frac{B_{u_1}}{A_{u_1}} + \sqrt{\left(\frac{B_{u_1}}{A_{u_1}}\right)^2 - \frac{C_{u_1}}{A_{u_1}}},$$

$$z^{max/min} = \frac{1}{2}(\tau + \sqrt{\tau^2 - 4m_l^2v}), \quad \tau = s - v - m_l^2.$$

During the calculation we used the abbreviations

$$\begin{aligned} t_{\Gamma w}^2 &= t_w^2 + m_W^2 \Gamma_W^2, \quad t_{\Gamma w} = \sqrt{t_{\Gamma w}^2}, \\ T_u &= m_W^2(v-u) + su, \quad T_{\Gamma u}^2 = T_u^2 + (v-u)^2 m_W^2 \Gamma_W^2, \\ T_t &= m_W^2(v-t) + st, \quad T_{\Gamma t}^2 = T_t^2 + (v-t)^2 m_W^2 \Gamma_W^2. \end{aligned} \quad (3)$$

and following list of integrals over u_1 :

$$\begin{aligned} J_1 &= \frac{1}{\pi} \int_{u_1^{min}}^{u_1^{max}} \frac{u_1^2 du_1}{\sqrt{R_{u_1}}} = \frac{3B_{u_1}^2 - A_{u_1} C_{u_1}}{2A_{u_1}^{5/2}}, \\ J_2 &= \frac{1}{\pi} \int_{u_1^{min}}^{u_1^{max}} \frac{u_1 du_1}{\sqrt{R_{u_1}}} = -\frac{B_{u_1}}{A_{u_1}^{3/2}}, \\ J_3 &= \frac{1}{\pi} \int_{u_1^{min}}^{u_1^{max}} \frac{du_1}{\sqrt{R_{u_1}}} = \frac{1}{\sqrt{A_{u_1}}}, \\ J_4 &= \frac{1}{\pi} \int_{u_1^{min}}^{u_1^{max}} \frac{du_1}{u_1 \sqrt{R_{u_1}}} = \frac{1}{\sqrt{C_{u_1}}}, \\ J_5 &= \frac{1}{\pi} \int_{u_1^{min}}^{u_1^{max}} \frac{du_1}{u_1^2 \sqrt{R_{u_1}}} = -\frac{B_{u_1}}{C_{u_1}^{3/2}}, \\ J_6 &= \frac{1}{\pi} \int_{u_1^{min}}^{u_1^{max}} \frac{du_1}{z_1 \sqrt{R_{u_1}}} = \frac{1}{\sqrt{C_{z_1}}}, \\ J_7 &= \frac{1}{\pi} \int_{u_1^{min}}^{u_1^{max}} \frac{du_1}{z_1^2 \sqrt{R_{u_1}}} = -\frac{B_{z_1}}{C_{z_1}^{3/2}}, \end{aligned} \quad (4)$$

where

$$\begin{aligned} B_{z_1} &= -A_{u_1}(v+z) - B_{u_1}, \\ C_{z_1} &= A_{u_1}(v+z)^2 + 2B_{u_1}(v+z) + C_{u_1}. \end{aligned} \quad (5)$$

At last, we list the following table of scalar integrals (W -boson width is neglected where it is possible)

$$I_1 = I[1] = 1,$$

$$\begin{aligned}
I_2 &= I\left[\frac{1}{z}\right] = \frac{\log[(s-v)^2/m_l^2 v]}{s-v}, \\
I_3 &= I\left[\frac{1}{u_1}\right] = \frac{\log[(s+u)^2/m_2^2 v]}{s+u}, \\
I_4 &= m_l^2 I\left[\frac{u_1}{z^2}\right] = -\frac{u}{s-v}, \\
I_5 &= m_2^2 I\left[\frac{1}{u_1^2}\right] = \frac{1}{v}, \\
I_6 &= I[u_1] = \frac{1}{2}(s+u), \\
I_7 &= I\left[\frac{u_1}{z}\right] = \frac{uv(1-\log[(s-v)^2/m_l^2 v])-st}{(s-v)^2}, \\
I_8 &= I\left[\frac{1}{zz_1}\right] = -\frac{1}{vt} \log \frac{t^2}{m_1^2 m_l^2}, \\
I_9 &= I\left[\frac{1}{zu_1}\right] = -\frac{1}{vu} \log \frac{u^2}{m_2^2 m_l^2}, \\
I_{10} &= I\left[\frac{u_1^2}{z}\right] = \frac{u^2 v^2}{(s-v)^3} \log\left[\frac{(s-v)^2}{m_l^2 v}\right] \\
&\quad + \frac{s^2 t^2 + 4uvst - 3u^2 v^2}{2(s-v)^3}, \\
I_{11} &= m_l^2 I\left[\frac{u_1^2}{z^2}\right] = \frac{vu^2}{(s-v)^2}, \tag{6}
\end{aligned}$$

$$\begin{aligned}
I_{12} &= ReI[\Pi_q] = -\frac{1}{(s-v)} \log\left[\frac{t_{\Gamma_W}}{m_W^2}\right], \\
I_{13} &= ReI\left[\frac{\Pi_q}{z_1}\right] = \frac{T_u}{T_{\Gamma_u}^2} \log\left[\frac{T_{\Gamma_u}^2}{m_1^2 m_W^2 t_{\Gamma_W} v}\right], \\
I_{14} &= ReI[u_1 \Pi_q] = \frac{(uv-st)}{(s-v)^2} + \frac{(m_w^2 uv - st t_w)}{(s-v)^3} \log\left[\frac{t_{\Gamma_W}}{m_W^2}\right], \\
I_{15} &= ReI[u_1^2 \Pi_q] = \frac{3s^2 t^2 - 4stuv - u^2 v^2}{2(s-v)^3}
\end{aligned}$$

$$\begin{aligned}
& -\frac{s^2 t^2 - 4 s t u v + u^2 v^2}{(s-v)^4} m_W^2 \\
& + \frac{2 m_W^2 t_w s t v u - (s t t_w - m_W^2 u v)^2}{(s-v)^5} \log \left[\frac{t_{\Gamma w}}{m_W^2} \right], \\
I_{16} &= ReI\left[\frac{\Pi_q}{u_1}\right] = I_{13}\{m_1 \rightarrow m_2, u \leftrightarrow t\}, \\
I_{17} &= m_2^2 ReI\left[\frac{\Pi_q}{u_1^2}\right] = \frac{(v-t)T_t}{vT_{\Gamma t}^2}, \\
I_{18} &= I[\Pi_q \Pi_q^+] = \frac{\pi/2 - \arctan(t_w/(m_W \Gamma_W)) - \arctan(\Gamma_W/m_W)}{m_W \Gamma_W (s-v)}, \\
I_{19} &= I\left[\frac{1}{z_1} \Pi_q \Pi_q^+\right] = \frac{1}{T_{\Gamma u}^2} \left[-\frac{T_u}{m_W \Gamma_W} \left(\arctan \left[\frac{(s-m_W^2)m_W}{s \Gamma_W} \right] \right. \right. \\
& \left. \left. - \arctan \left[\frac{(s-m_W^2)T_u}{v s m_W \Gamma_W} \right] \right) + (s+t) \log \left[\frac{|u| \sqrt{T_{\Gamma u}^2}}{m_1^2 m_W^2 v} \right] \right], \\
I_{20} &= I\left[\frac{1}{u_1} \Pi_q \Pi_q^+\right] = I_{19}\{m_1^2 \rightarrow m_2^2, t \leftrightarrow u\}, \\
I_{21} &= m_1^2 I\left[\frac{1}{z_1^2} (\Pi_q \Pi_q^+ - \Pi_l \Pi_l^+)\right] = (s(v-2u) + 2m_W^2(u-2v)) s \Pi_l \Pi_l^+ / T_{\Gamma u}^2, \\
I_{22} &= m_2^2 I\left[\frac{1}{u_1^2} \Pi_q \Pi_q^+\right] = \frac{(s+u)^2}{v T_{\Gamma t}^2}, \\
I_{23} &= I[u_1 \Pi_q \Pi_q^+] = \frac{1}{(s-v)^3} \left[(s t - u v) \log \frac{t_{\Gamma w}}{m_W^2} \right. \\
& \left. + \frac{t_w s t - m_W^2 u v}{m_W^2} \left(\frac{m_W}{\Gamma_W} \left(\pi/2 - \arctan \left[\frac{t_w}{\Gamma_W m_W} \right] \right) - 1 \right) \right], \\
I_{24} &= I[u_1^2 \Pi_q \Pi_q^+] = \frac{1}{(s-v)^5} \left[\frac{(\pi - 2 \arctan[t_w/(m_W \Gamma_W)])}{4 m_W \Gamma_W} \right. \\
& \times [3(s t t_w - m_W^2 u v)^2 - (s t + m_W^2(s+u))^2(s-v)^2] \\
& \left. + s^2 t^2 \left(s - v - \frac{t_w^2}{m_W^2} \right) - 4(s-v-t_w) s t u v - t_w u^2 v^2 \right]
\end{aligned}$$

$$\begin{aligned}
& + [t_w s^2 t^2 - 2s t u v (t_w + m_W^2) + m_W^2 u^2 v^2] \log \left[\frac{t_{\Gamma_w}^2}{m_W^4} \right], \\
I_{25} &= I \left[\frac{\Pi_q \Pi_q^+}{z_1(z+v)} \right] = \frac{1}{T_{\Gamma_u}^2} \left[\frac{(v-u)^2}{sv} \log \frac{s}{m_1^2} \right. \\
& + (vs - 2(s+t)(s-m_W^2)) \Pi_l \Pi_l^+ \log \frac{v m_W^2}{\sqrt{T_{\Gamma_u}^2}} \\
& - \frac{vs - (s+t)(s-m_W^2)}{m_W \Gamma_W} (s-m_W^2) \Pi_l \Pi_l^+ \\
& \times \left. \left(\arctan \left[\frac{(s-m_W^2)m_W}{s \Gamma_W} \right] - \arctan \left[\frac{(s-m_W^2)T_u}{v s m_W \Gamma_W} \right] \right) \right], \\
I_{26} &= I \left[\frac{\Pi_q \Pi_q^+}{u_1(z+v)} \right] = I_{25} \{m_1^2 \rightarrow m_2^2, t \leftrightarrow u\}, \\
I_{27} &= I \left[\frac{1}{z_1 u_1} \right] = \frac{1}{sv} \log \frac{s^2}{m_1^2 m_2^2}, \\
I_{28} &= I \left[\frac{1}{z_1} \right] = \frac{1}{v-u} \log \frac{(v-u)^2}{m_1^2 v}. \tag{8}
\end{aligned}$$

B Expressions for the V_j .

B.1 The case of $q\bar{q} \rightarrow l^-\bar{\nu}_l, \bar{q}q \rightarrow l^+\nu_l$ subprocesses

$$V_l = V_l^* = 4uI_4 - I_6 - uI_7 + I_{10} - 2I_{11} \tag{1}$$

$$\begin{aligned}
V_{lq} = V_{lq}^* &= Q_i \{ -(2u(u-t) + vt)I_2 + (u-t)(I_7 - I_{14}) \\
& + vt(2\Pi_l u^2 - 2u + v)I_8 - (t_w(s+u) - vt - 2u(u-t))I_{12} \\
& + (t_w(v-u)(v-2u) - t(2u^2 - 2uv + v^2))I_{13} \} / t_{w\Gamma} \\
& + Q_{i'} \{ 2t_w I_1 + 4u^2 I_2 - 2t_w I_3 - 2u I_7 - 2\Pi_l u^3 v I_9 \\
& - 2(t_w - u)((t_w - 2u)I_{12} + I_{14} - u(t_w - u)I_{16}) \} / t_{w\Gamma} \tag{2}
\end{aligned}$$

$$\begin{aligned}
V_q = V_q^* &= -Q_i^2 u \{ v I_{19} + 2u I_{21} \} + Q_{i'}^2 \{ -I_3 + 2(\Pi_l \Pi_l^+ u^2 - 1)I_5 + I_{12} \\
& + (2t_w - u)I_{16} + (t_w - u)(4I_{17} - t_w I_{20} - 2(t_w - u)I_{22}) \\
& - t_w I_{18} \} + Q_i Q_{i'} \{ (s-u)I_{16} - (s-v)I_{18} \\
& - (2u^2 - 3uv + v^2)I_{19} - ((s-u)(t_w - 2u) + sv)I_{20} \\
& + sv(v-2u)(I_{25} + I_{26}) + 2su^2(I_{25} + I_{26} - \Pi_l \Pi_l^+ I_{27}) \} \tag{3}
\end{aligned}$$

$$\begin{aligned}
V_{lw} = & \{st_w I_1 + 2su^2 I_2 + 2t_w I_6 - u(2s - v)I_7 + (s - v)I_{10} \\
& - (s(t_w - u)^2 + u(t_w(u - v) + su))I_{12} \\
& - (t_w - u)(2t_w + 2s - v)I_{14} - (s + 2t_w - v)I_{15}\} / t_w \Gamma
\end{aligned} \tag{4}$$

$$\begin{aligned}
V_{qw} = & Q_i \{sI_{12} - (2u^2 - 3uv + v^2)I_{13} + (s(2u - t_w) + u^2 + vt))I_{18} \\
& + ((t_w - v + s)(2u^2 - 3uv + v^2) + suv)I_{19} + tI_{23}\} \\
& + Q_{i'} \{-2I_1 - (s - u)I_3 + (2s + 4t_w - 4u - v)I_{12} + 2I_{14} \\
& + (uv + 2(t_w - u)(s - u))I_{16} \\
& + (t_w(4u + v - 2t_w - 2s) + u(2s - u - 3v))I_{18} \\
& - (t_wuv + (s - u)t_w(t_w - 2u) + 2u^2(s - v))I_{20} \\
& + (t - 2t_w + 2u)I_{23}\}
\end{aligned} \tag{5}$$

$$\begin{aligned}
V_w = & -sI_1 - I_6 + (2st_w - u(3s + t))I_{12} + (2s + 2t_w - u - v)I_{14} \\
& + I_{15} + (t_w(u(3s + t) - st_w) + u(uv - v^2 - 2su))I_{18} \\
& + (u(2s - v) + t_w(u + v - t_w - 2s))I_{23} - (s - v + t_w)I_{24}
\end{aligned} \tag{6}$$

B.2 The case of for $q\bar{q} \rightarrow l^+\nu_l, \bar{q}q \rightarrow l^-\bar{\nu}_l$ subprocesses

$$V_l = V_l^*(t \leftrightarrow u) \tag{7}$$

$$V_{lq} = V_{lq}^*(t \leftrightarrow u, m_1 \leftrightarrow m_2, Q_i \leftrightarrow Q_{i'}) \tag{8}$$

$$\begin{aligned}
V_q = & Q_i^2 \{I_{12} + (2t_w - t)I_{13} - t_w I_{18} + t_w(t - t_w)I_{19} \\
& - 2(t - t_w)^2 I_{21} - I_{28}\} + Q_{i'}^2 t \{2t\Pi_l\Pi_l^+ I_5 - vI_{20} - 2tI_{22}\} \\
& + Q_i Q_{i'} \{(s - t)I_{13} - (s - v)I_{18} \\
& + ((2t - t_w)(s - t) - sv)I_{19} - (2t^2 - 3tv + v^2)I_{20} \\
& + (2t^2 - 2tv + v^2)s(I_{25} + I_{26} - \Pi_l\Pi_l^+ I_{27}) \\
& + \Pi_l\Pi_l^+ sv(v - 2t)I_{27}\}
\end{aligned} \tag{9}$$

$$\begin{aligned}
V_{lw} = & \{2t_w(t - v)I_1 + (2st(t - v) - v^2u)I_2 + 2t_w I_6 \\
& + (2st + tv + 2vu)I_7 + (s - v)I_{10} \\
& + ((u - 3t_w)v^2 + 2(st + t_w^2)(v - t) + tt_w(4v - t))I_{12} \\
& + (2v(3t_w - u) - (t + t_w)(2t_w + v) - 2st)I_{14} \\
& - (s - v + 2t_w)I_{15}\} / t_w \Gamma
\end{aligned} \tag{10}$$

$$\begin{aligned}
V_{qw} = & Q_i \{ (s - 3t + 2v)I_{12} + (2(s - t)(t_w - t) + tv)I_{13} - 2I_{14} \\
& + (t(2s - t - v) - t_w(s - 3t + 2v) + vu)I_{18} \\
& + (t(2s + t_w - v)(t_w - t) - st_w^2 + t^2(v - t_w))I_{19} \\
& + (2t_w - 2t - u)I_{23} - (s - t)I_{28} \} + Q_{i'} \{ (v - t)I_{12} \\
& - (2t^2 - 3tv + v^2)I_{16} + (t(2s + t + t_w) + v(2u - t_w))I_{18} \\
& + ((s - v + t_w)(2t^2 + v^2) - tv(2s + 3(t_w - v)))I_{20} - uI_{23} \}
\end{aligned} \tag{11}$$

$$\begin{aligned}
V_w = & (v - t)I_1 - I_6 + (2t_w(t - v) + t^2 - 3tv + 2v^2)I_{12} \\
& + (t + 2t_w - 3v)I_{14} + I_{15} \\
& + ((v - t - t_w)(v - t)(v - t_w) - s(2t(t - v) + v^2))I_{18} \\
& + ((2s + t)(v - t) - t_w^2 + 3t_wv - 2v^2)I_{23} - (s - v + t_w)I_{24}
\end{aligned} \tag{12}$$

References

1. J. Ashman et al. Phys. Lett. B **206** (1988) 364; J. Ashman et al. Nucl. Phys. B **328** (1989) 1
2. B. Adeva et al. Phys. Rev. D **58** (1998) 112001
3. (E142) P.L. Anthony et al. Phys. Rev. D **54** (1996) 6620; (E143) K. Abe et al. Phys. Rev. D **58** (1998) 112003; (E154) K. Abe et al. Phys. Rev. Lett. **79** (1997) 26; (E155) P.L. Anthony et al. Phys. Lett. B **493** (2000) 19
4. A. Airapetian et al. Phys. Rev. Lett. **84** (2000) 2584
5. (SMC) B. Adeva et al. Phys. Lett. B **420** (1998) 180
6. (HERMES) K. Ackerstaff et al. Phys. Lett. B **464** (1999) 123
7. RSC Coll. Proposal on spin Physics using the RHIC Polarized Collider. (1992), August; G. Bunce et al. Ann. Rev. Nucl. Part. Sci. **50** (2000) 525
8. "Acceleration of polarized protons to 120 GeV and 1TeV at Fermilab", Univ. of Michigan, (1995), July *HE 95-09*
9. W.-D Nowak (1996) DESY 96-095
10. C. Bourrely et al. Phys. Rept. **177** (1989) 319
11. I.V. Akushevich, N.M. Shumeiko J. Phys. G **20** (1994) 513
12. N.M. Shumeiko, S.I. Timoshin, V.A. Zykunov J.Phys G **23** (1997) 1593
13. F. Berends, R. Kleiss Z. Phys. C **27** (1985) 365
14. U. Baur, S. Keller, D. Wackerlohe Phys. Rev. D **59** (1999) 013002
15. D.Yu. Bardin et al. Preprint JINR E2-87-595 Dubna (1987)
16. M. Böhm, H. Spiesberger Nucl. Phys. B **294** (1987) 1081
17. M. Böhm, H. Spiesberger Nucl.Phys. B **304** (1988) 749
18. V.A. Zykunov, S.I. Timoshin, N.M. Shumeiko Yad.Fiz **58** (1995) 2021 (Engl. Transl.: Phys. of Atom. Nuclei **58** (1995) 1911)
19. D.Yu. Bardin, N.M. Shumeiko Nucl.Phys. B **127** (1977) 242; Sov. J. Nucl. Phys. **29** (1979) 969
20. M. Böhm et al. Forschr.Phys. **34** (1986) 687
21. A.D. Martin et al. August *Durham preprint DTP/98/52* (1998)
22. M. Gluck et al. *DESY 94-206* (1994)
23. M. Gluck et al. Phys. Rev. D **53** (1996) 4775

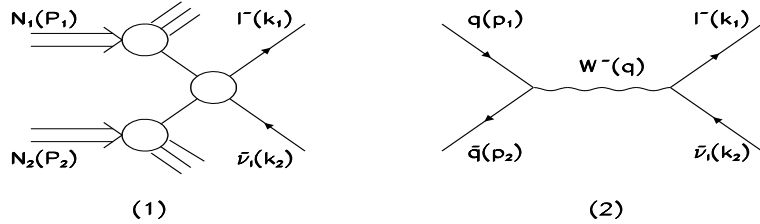


Fig. 1. (1) Sketch illustrating the interaction of parton 1 and 2 from incident nucleons N_1 and N_2 , respectively. The partons carry fractional momenta x_1 and x_2 and interact to produce a charged lepton and antineutrino. (2) The diagram for the lowest order subprocess $q\bar{q} \rightarrow l^-\bar{\nu}$.

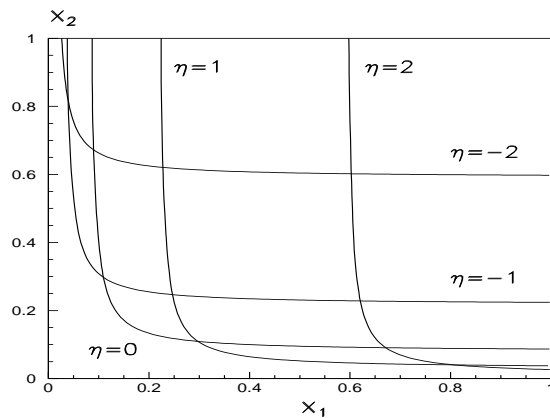


Fig. 2. Physically allowed region of variables x_1 and x_2 . Curves on the plot are x_2^0 as a function of x_1 at different η (kinematics of RHIC experiment STAR: $\sqrt{S}=500$ GeV, $k_{1\perp}=40$ GeV).

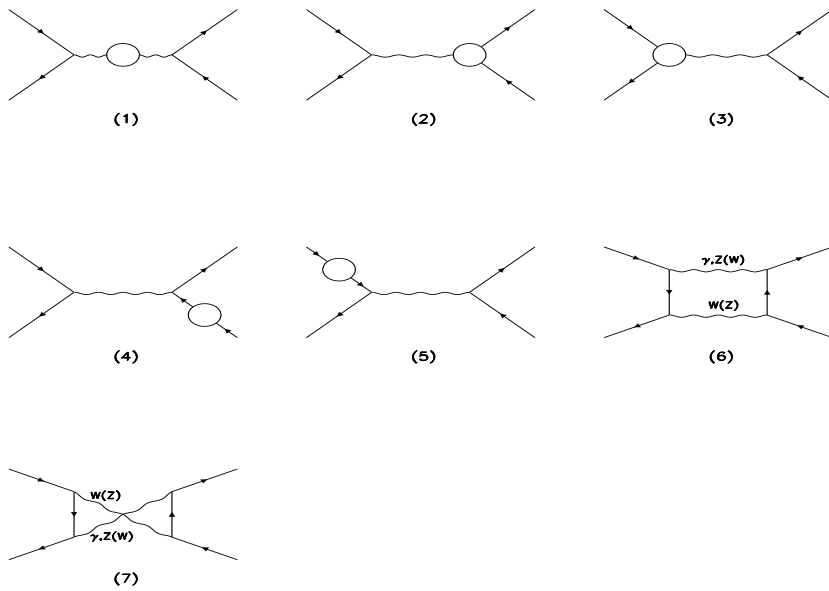


Fig. 3. The virtual one-loop diagrams for $q\bar{q} \rightarrow l^-\bar{\nu}$ process. The contributions to the self-energies and vertex corrections are symbolized by the empty loops, an explicit representation can be found in Ref.[17].

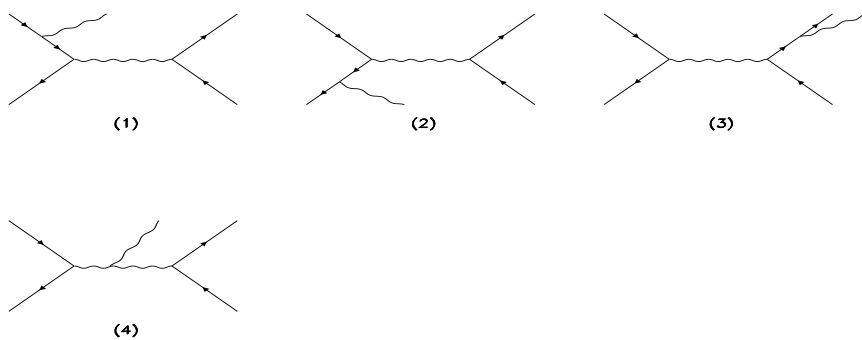


Fig. 4. Bremsstrahlung diagrams for $q\bar{q} \rightarrow l^-\bar{\nu}\gamma$ process.

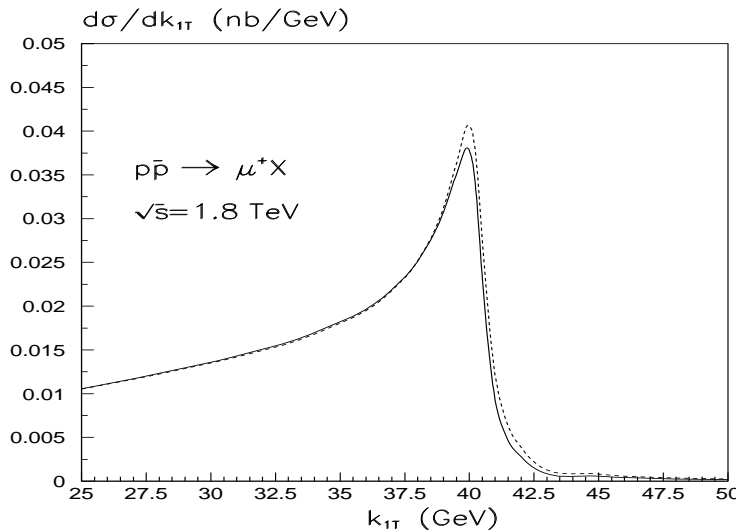


Fig. 5. Differential cross sections for $p\bar{p} \rightarrow \mu^+X$ at $\sqrt{S} = 1.8$ TeV, $-1.2 \leq \eta \leq 1.2$, $\Delta\Phi = 2\pi$ (Tevatron) as a function of k_{1T} . Shown is the muon transverse momentum spectrum in the Born approximation (dashed line) and taking into account the total EWC (solid line). We use the MRS LO 98 set of parton distribution functions [21].

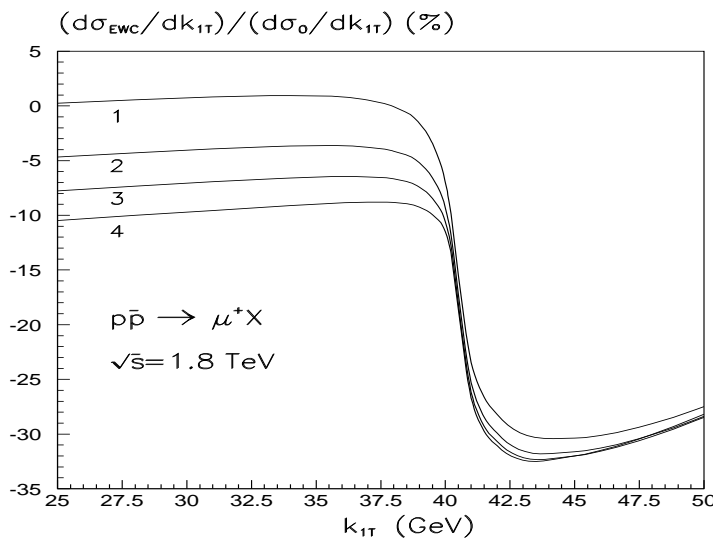


Fig. 6. The ratio of the $O(\alpha^3)$ and the Born cross sections as a function of k_{1T} at different values of quark masses: $m_u=5 \text{ MeV}$, $m_d=8 \text{ MeV}$ (curve 1), $m_u=30 \text{ MeV}$, $m_d=30 \text{ MeV}$ (curve 2), $m_u=100 \text{ MeV}$, $m_d=100 \text{ MeV}$ (curve 3), $m_u=0.33 \text{ GeV}$, $m_d=0.33 \text{ GeV}$ (curve 4). The rest of the parameters is identical to that in Fig. 5.

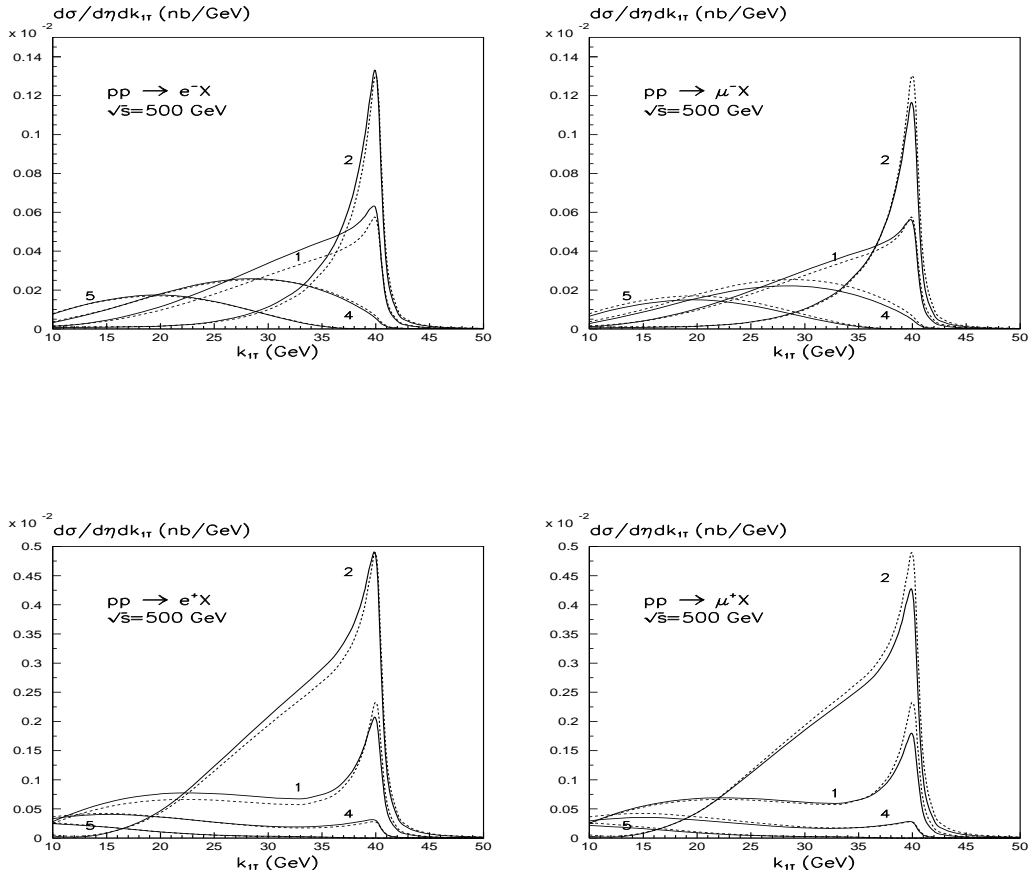


Fig. 7. Spin averaged part of the double differential cross sections for $p\bar{p} \rightarrow l^\pm X$ at $\sqrt{S} = 500$ GeV, $\Delta\Phi = 2\pi$ (RHIC) as a function of k_{1T} for the pseudo-rapidity $\eta = -1$ (curve 1), $\eta = 0$ (curve 2), $\eta = 1.5$ (curve 4), $\eta = 2$ (curve 5) in the case of e^\pm , μ^\pm final states. Shown on the figures are the cross sections in the Born approximation (dashed lines) and taking into account the total EWC (solid lines). We use the GRV94 proton parametrization of parton distribution functions [22].

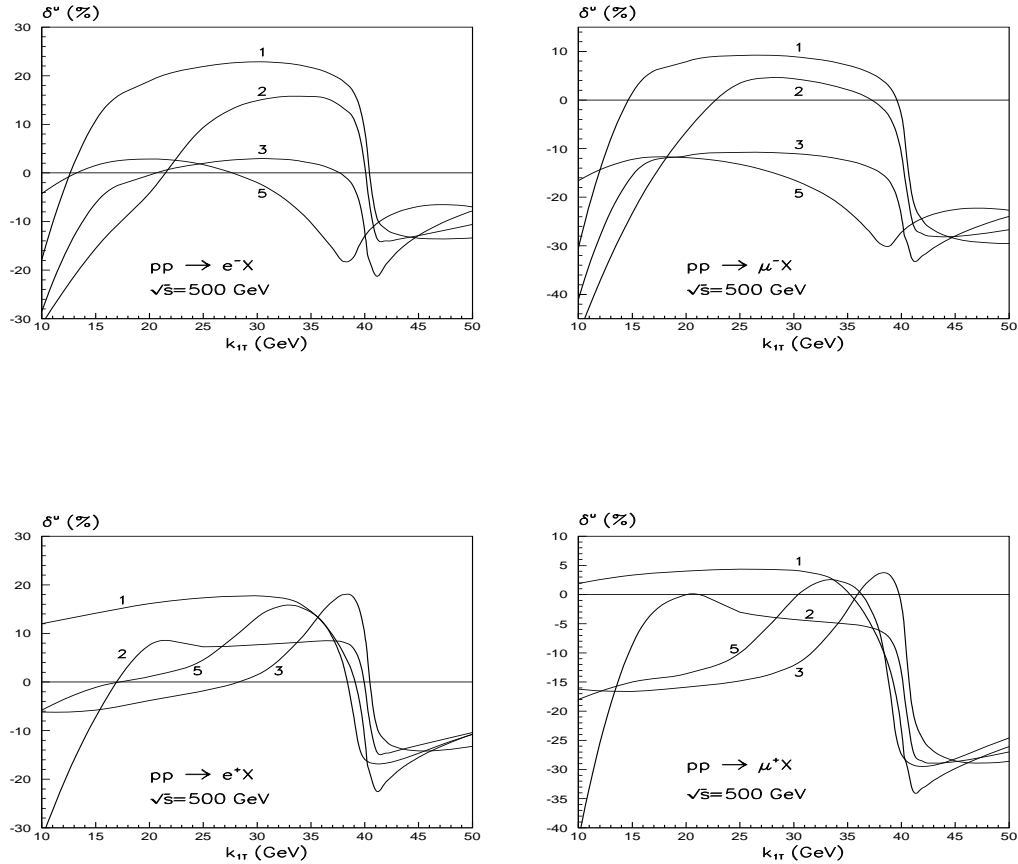


Fig. 8. Corrections δ^u for $p\bar{p} \rightarrow l^\pm X$ at RHIC kinematics as a function of k_{1T} for the pseudo-rapidity $\eta = -1$ (curve 1), $\eta = 0$ (curve 2), $\eta = 1$ (curve 3), $\eta = 2$ (curve 5) in the case of e^\pm, μ^\pm final states. The rest of the parameters is identical to that in Fig. 7.

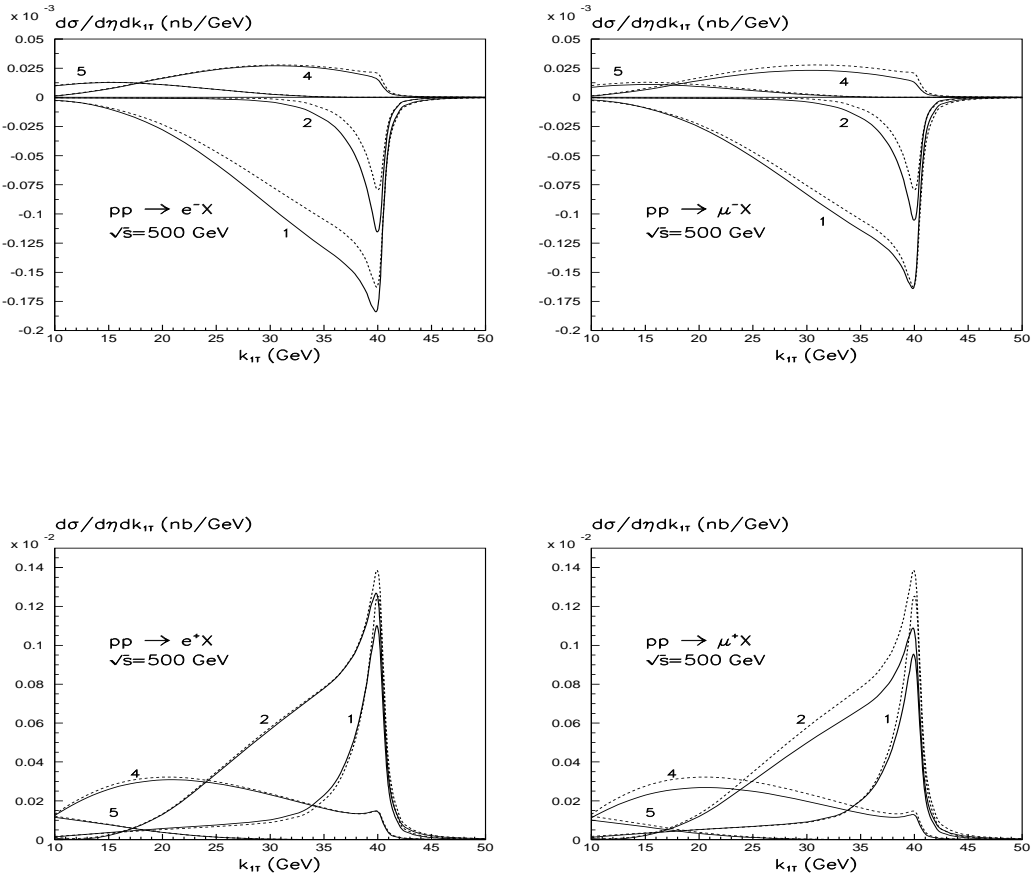


Fig. 9. Polarization part of the double differential cross sections for $p\bar{p} \rightarrow l^\pm X$ at $\sqrt{S} = 500$ GeV, $\Delta\Phi = 2\pi$ (RHIC) as a function of k_{1T} for the pseudo-rapidity $\eta = -1$ (curve 1), $\eta = 0$ (curve 2), $\eta = 1.5$ (curve 4), $\eta = 2$ (curve 5) in the case of e^\pm, μ^\pm final states. Shown on the figures are the cross sections in the Born approximation (dashed lines) and taking into account the total EWC (solid lines). We use the GRSV96 LO proton parametrization of polarized parton distribution functions [23].

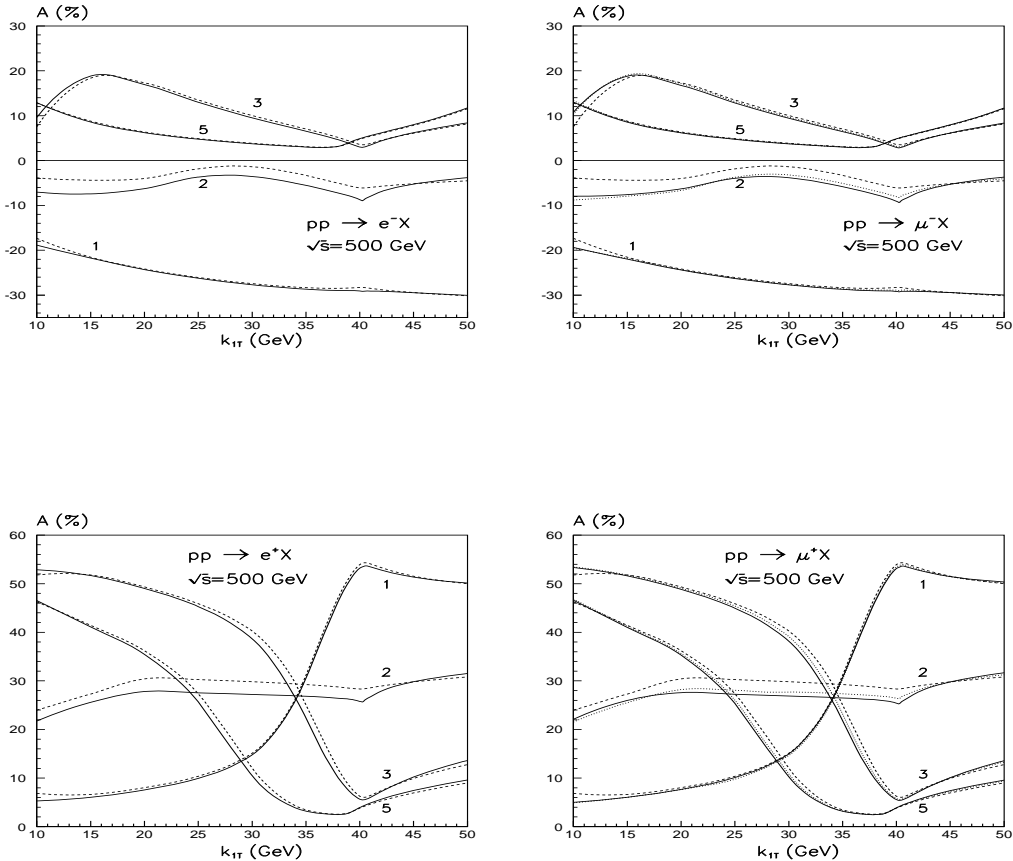


Fig. 10. Single spin asymmetries for $p\bar{p} \rightarrow l^\pm X$ at RHIC kinematics as a function of k_{1T} for the pseudo-rapidity $\eta = -1$ (curve 1), $\eta = 0$ (curve 2), $\eta = 1$ (curve 3), $\eta = 2$ (curve 5) in the Born approximation (dashed lines) and taking into account the total EWC: solid lines for the current quark masses, and dotted lines for the extreme choice $m_u = m_d = 0.33$ GeV. The rest of the parameters is identical to that in Fig. 9.